Bifurcation analysis of the attitude dynamics for a magnetically controlled spacecraft

Fabio Della Rossa, Marco Bergamasco and Marco Lovera

***Abstract*— The dynamics of a spacecraft equipped with magnetic actuators operating under a static attitude and rate feedback control law designed using averaging theory is considered and the asymptotic behaviour of the closed-loop system as a function of the averaging scaling parameter is analysed, using bifurcation methods.**

I. INTRODUCTION

The problem of attitude control of rigid spacecraft equipped with magnetic actuators has been widely studied in recent years (see, *e.g.*, the survey paper [20]). The main difficulty in this problem is due to the principle of operation of such actuators. Indeed, magnetic coils generate control torques by interacting with the magnetic field of the Earth and this has a number of implications which make the magnetic attitude control problem significantly different from the conventional one. First of all, it is not possible by means of such actuators to provide three independent control torques at each time instant. In addition, the behaviour of these actuators is time-varying (periodically forced), as the control mechanism hinges on the variations of the Earth magnetic field along the spacecraft orbit. Nevertheless, attitude stabilisation is possible because *on average* the system possesses strong controllability properties for a wide range of orbit inclinations (see also [4]).

A significant effort has been dedicated in recent years to the problems of analysis and design of magnetic control laws in the linear case, *i.e.*, control laws for *local* operation of a satellite near a constant reference attitude. In particular, nominal and robust stability and performance have been studied, using mainly tools from periodic control theory exploiting the (quasi) periodic behavior of the system near an equilibrium (see, *e.g.*, [17], [19], [24], [25]).

Similarly, attention has been dedicated to *global* formulations of the problem. In [23], [7], [2] the attitude regulation problem for Earth pointing spacecraft has been addressed exploiting periodicity assumptions on the system and resorting to passivity arguments to prove local asymptotic stabilisability of stable open-loop equilibria. In [21] similar arguments have been used to study a state feedback control law for the particular case of an inertially spherical spacecraft. More recently, in [15] (resp. [16]) stability conditions for state feedback control laws achieving inertial pointing (resp. Earth pointing) for magnetically actuated spacecraft have been presented. The above mentioned results concerning almost global[1] stabilisation using magnetic actuators have been derived by resorting to averaging theory, *i.e.*, by associating to the time-varying dynamics of the magnetically controlled spacecraft a suitably defined time-averaged counterpart and showing that for sufficiently small values of a scaling parameter ε the trajectories of the former can be approximated by the ones of the latter. This result provides an interesting characterisation of the global properties of magnetic state feedback controllers, but leaves open the problem of characterising the range of values of the scaling parameter for which the result actually holds.

In view of the above discussion, the aim of this paper is to investigate the dynamics of a magnetically actuated spacecraft operating under the state feedback control law of [15], for increasing values of the scaling parameter ε. The tools employed in the study are Floquet theory for the asymptotic stability analysis of the linearised model and bifurcation theory (see, *e.g.*, [18] and the references therein) for larger values of the parameter. Note, in passing, that while a few analyses based on bifurcation theory for the dynamics of a rigid spacecraft immersed in a central gravitational field can be found in the literature (see, *e.g.*, [12], [13]), as far as the interaction with the geomagnetic field is concerned it appears that only the case of a spacecraft with a constant residual magnetic dipole has been studied (see [6]), while the case of magnetic feedback control is an open problem.

II. SPACECRAFT MODEL

In the following we will focus on the case of an inertially pointing spacecraft, for modelling which the following reference systems have to be defined.

- Earth Centered Inertial reference frame (ECI). The origin of this reference frame is in the Earth's centre. The X-axis is parallel to the line of nodes (*i.e.*, the intersection between the Earth's equatorial plane and the plane of the ecliptic) and is positive in the Vernal equinox direction (Aries point). The Z-axis is defined as parallel to the Earth's geographic north-south axis, pointing north. The Y-axis completes the right-handed orthogonal triad.
- Satellite body reference frame. The origin of this frame is in the satellite centre of mass; for the sake of simplicity the axes are assumed to coincide with the body's principal inertia axes.

F. Della Rossa, M. Bergamasco and M. Lovera are with the Dipartimento di Elettronica e Informazione, Politecnico di Milano Piazza Leonardo da Vinci 32, 20133 Milano, Italy {dellarossa,bergamasco,lovera}@elet.polimi.it

[1]Given a system $\dot{x} = f(x)$ we say that an equilibrium x_0 is almost globally asymptotically stable if it is locally asymptotically stable, all the trajectories of the system are bounded and the set of initial conditions giving rise to trajectories which do not converge to x_0 has zero Lebesgue measure.

The attitude dynamics can be expressed by Euler's equations as [22]

$$I\dot{\omega} = S(\omega)I\omega + T_{coils} + T_{dist} \tag{1}$$

where $\omega \in \mathbb{R}^3$ is the vector of spacecraft angular rates, in the body frame, $I \in \mathbb{R}^{3\times 3}$ is the inertia matrix, and $S(\omega)$ is given by

$$S(\omega) = \begin{bmatrix} 0 & \omega_z & -\omega_y \\ -\omega_z & 0 & \omega_x \\ \omega_y & -\omega_x & 0 \end{bmatrix}, \tag{2}$$

$T_{coils} \in \mathbb{R}^3$ is the vector of external torques induced by the magnetic coils and $T_{dist} \in \mathbb{R}^3$ is the vector of external disturbance torques.

As for the attitude kinematics, a number of possible parameterisations (see, *e.g.*, [22]) can be adopted. A frequently adopted parameterisation is given by the four Euler parameters (or quaternions), which lead to the following representation for the attitude kinematics

$$\dot{\boldsymbol{q}} = W(\boldsymbol{q})\omega \tag{3}$$

where $\boldsymbol{q} = \begin{bmatrix} q_1 & q_2 & q_3 & q_4 \end{bmatrix}^T = \begin{bmatrix} \mathbf{q}^T & q_4 \end{bmatrix}^T$ is the vector of unit norm ($\boldsymbol{q}^T\boldsymbol{q} = 1$) Euler parameters and

$$W(\boldsymbol{q}) = \frac{1}{2}\begin{bmatrix} q_4 & -q_3 & q_2 \\ q_3 & q_4 & -q_1 \\ -q_2 & q_1 & q_4 \\ -q_1 & -q_2 & -q_3 \end{bmatrix}, \tag{4}$$

i.e., the attitude of the inertially pointing spacecraft is referred to the ECI reference frame.

The available on-board actuators are a set of three magnetic coils, aligned with the spacecraft body axes, which generate torques according to the law

$$T_{coils} = m_{coils} \times \tilde{b}(t) = S(\tilde{b}(t))m_{coils}, \tag{5}$$

where $\times$ denotes the vector cross product, $m_{coils} \in \mathbb{R}^3$ is the vector of magnetic dipoles for the three coils (which represent the actual control variables for the coils), $\tilde{b}(t) \in \mathbb{R}^3$ is the vector formed with the components of the Earth's magnetic field in the body frame of reference. Note that the vector $\tilde{b}(t)$ can be expressed in terms of the attitude matrix $A(\boldsymbol{q})$ (see [22] for details) and of the magnetic field vector expressed in the ECI coordinates, namely $\tilde{b}_0(t)$, as

$$\tilde{b}(t) = A(\boldsymbol{q})\tilde{b}_0(t), \tag{6}$$

and that the orthogonality of $A(\boldsymbol{q})$ implies $\|\tilde{b}(t)\| = \|\tilde{b}_0(t)\|$. Since rank $\Big(S(\tilde{b}(t))\Big) = 2$ ($\|\tilde{b}_0(t)\| \neq 0$ along all orbits of practical interest for magnetic control), magnetic actuators do not provide complete controllability of the system at each time instant. In particular, the kernel of $S(\tilde{b}(t))$ is given by the vector $\tilde{b}(t)$ itself, *i.e.*, at each time instant it is *not* possible to apply a control torque along the direction of $\tilde{b}(t)$.

In the following so-called "projection-based" magnetic controllers will be considered, *i.e.*, the preliminary feedback

$$m_{coils} = \frac{1}{\|\tilde{b}_0(t)\|^2} S^T(\tilde{b}(t))u \tag{7}$$

is applied to the system, where $u \in \mathbb{R}^3$ is a new control vector. Then the overall dynamics can be written as

$$\begin{array}{rcl} \dot{\boldsymbol{q}} & = & W(\boldsymbol{q})\omega \\ I\dot{\omega} & = & S(\omega)I\omega + \Gamma(t)u \end{array} \tag{8}$$

where $\Gamma(t) = S(b(t))S^T(b(t)) \geq 0$ and $b(t) = \frac{1}{\|\tilde{b}_0(t)\|}\tilde{b}(t) = \frac{1}{\|\tilde{b}(t)\|}\tilde{b}(t)$. Similarly, let $\Gamma_0(t) = S(b_0(t))S^T(b_0(t)) \geq 0$ and $b_0(t) = \frac{1}{\|\tilde{b}_0(t)\|}\tilde{b}_0(t)$.

Finally, for the geomagnetic field the tilted dipole model will be used in the following (see, *e.g.*, [22]). This model can be in turn approximated with a time-periodic function (with angular frequency $\omega = 2\omega_0$, ω_0 being the orbital angular frequency) provided that timescales shorter that the Earth rotation period are considered.

Remark 1: In the following we will assume that the considered orbit for the spacecraft satisfies the condition

$$\bar{\Gamma}_0 = \lim_{T\to\infty}\frac{1}{T}\int_0^T \Gamma_0(t)dt = \\ = \lim_{T\to\infty}\frac{1}{T}\int_0^T S(b_0(t))S^T(b_0(t))dt > 0.$$

This assumption is satisfied for most orbits of practical interest for low Earth orbit spacecraft.

III. STATE FEEDBACK STABILISATION

In this Section the general stabilisation result for a spacecraft with magnetic actuators given in [15] for the case of full state feedback (attitude and rate) is recalled. Without loss of generality in the following we assume that the equilibrium to be stabilised is given by $(\bar{\boldsymbol{q}}, 0)$, where $\bar{\boldsymbol{q}} = \begin{bmatrix} 0 & 0 & 0 & 1 \end{bmatrix}^T$.

Proposition 1: Consider the magnetically actuated spacecraft described by (8) and the control law

$$u = -I^{-1}(\varepsilon^2 k_p \mathbf{q} + \varepsilon k_v \omega), \tag{9}$$

with $k_p > 0$ and $k_v > 0$. Then there exists $\varepsilon^\star > 0$ such that for any $0 < \varepsilon < \varepsilon^\star$ the control law (9) ensures that $(\bar{\boldsymbol{q}}, 0)$ is a locally exponentially stable equilibrium for the closed loop system (8)-(9). Moreover, all trajectories of (8)-(9) are such that $\mathbf{q} \to 0$ and $\omega \to 0$.

Proof: See [15]. ■

Proposition 1 shows that for magnetic attitude control the proportional and derivative actions must meet the scaling condition defined by (9) to guarantee closed-loop stability. In this respect, this result provides a very useful guideline for the design of magnetic controllers in practical cases, as it combines the simplicity of a state feedback control law with an explicit stability condition. On the other hand, the choice of a suitable value for ε cannot be carried out on the basis of Proposition 1 only, but requires some additional methods and tools, which will be discussed in the following Sections.

In particular, in order to deal with the periodically forced (*i.e.*, nonautonomous) nature of the closed-loop system, Floquet theory will be used in Section IV for the local analysis (*i.e.*, based on the linear approximation of the closed-loop system around the equilibrium $(\bar{\boldsymbol{q}}, 0)$) while a more general investigation will be carried out in Section V using continuation methods for nonautonomous systems.

IV. LOCAL STABILITY ANALYSIS

A first approach to the problem of assessing the range of values of ε for which Proposition 1 holds is based on a local analysis of the closed-loop system (8)-(9). The linear approximation of the closed-loop system around the equilibrium $(\bar{\boldsymbol{q}}, 0)$ can be written as

$$\begin{array}{rcl} \dot{\mathbf{q}} & = & \frac{1}{2}\omega \\ I\dot{\omega} & = & -\Gamma_0(t) I^{-1}(\varepsilon^2 k_p \mathbf{q} + \varepsilon k_v \omega). \end{array} \tag{10}$$

System (10) is linear time-periodic and its stability can be therefore studied using Floquet theory (see, *e.g.*, [5]).

As an example, in Figure 1 the evolution of the real part of the characteristic exponents of system (10) as a function of ε is illustrated for the numerical example discussed in greater detail in Section VI. As can be seen from the Figure, one of

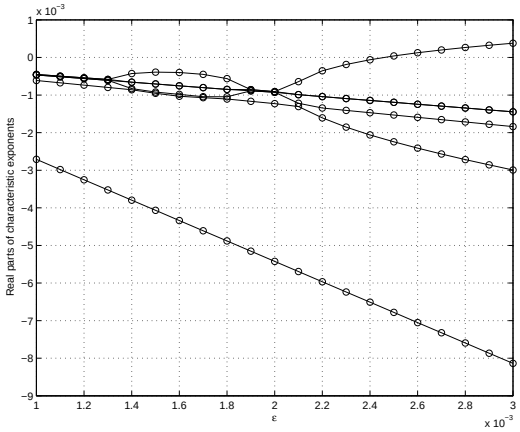

Fig. 1. Real parts of closed-loop characteristic exponents as a function of ε.

the characteristic exponents approaches the imaginary axis for increasing values of ε and eventually crosses it for $\varepsilon \simeq 0.0024$. While this analysis already provides some insight into the problem of choosing the value of ε in the control law (9), in the following Section a more general approach to the problem will be followed, based on bifurcation analysis.

V. BIFURCATION ANALYSIS

Equations (8)-(9) define a parameter-dependent family of dynamical systems. Parameter ε plays a key role in determining both stability and performance of the magnetic controller. In order to get a more general view on the behavior of the closed-loop system for different values of this parameter, we apply bifurcation analysis [18]. Indeed, this approach allows one to work out the catalogue of the qualitative behaviors of the system, together with the regions, delimited in parameter space by bifurcations, where the different behaviors occur. Although one might hope to detect bifurcations by simulating, *e.g.*, system (8)-(9), for various combinations of parameter and initial conditions, such a brute force approach is hardly effective and accurate in practice. This because bifurcations of equilibria and cycles are associated with a loss of stability, so that one should dramatically increase the duration of simulations while approaching the bifurcation. In particular, saddle sets, which are hard to find by simulation, play a fundamental role in bifurcation analysis, since they, together with attracting and repelling sets, define the structure of the phase portrait. This is why numerical bifurcation analysis does not rely on simulation, but rather on continuation (see [9], [1]), a numerical method suited for computing (approximating through a discrete sequence of points) one-dimensional manifolds implicitly defined as the zero set of a suitable function. The general idea is to formulate the computation of equilibria and their bifurcations as a suitable algebraic problem of the form

$$F(u, p) = 0, \tag{11}$$

where u is composed of the system's state and possibly other variables characterizing the system and p is the parameter vector. Problem (11) is defined by n equations and $n+1$ free variables (including parameters): knowing a point satisfying (11), the Implicit Function Theorem can be applied, allowing the explicit solution of the system as a function of the free parameter. This approach however is directly applicable only in the case of autonomous systems. In order to deal with nonautonomous systems, such as (8)-(9), some additional issues have to be dealt with, which are discussed in the following subsection.

A. Continuation of nonautonomous systems solutions

For the specific case of nonautonomous systems, the continuation approach outlined above calls for some preliminary modification to the system in order to work out an equivalent autonomous representation. This can be achieved by *bordering* the nonautonomous system with two additional variables described by the dynamical system

$$\begin{array}{rcl} \dot{\alpha} & = & \alpha - \omega\beta + (\alpha^2 + \beta^2)\alpha, \\ \dot{\beta} & = & \omega\alpha + \beta + (\alpha^2 + \beta^2)\beta. \end{array} \tag{12}$$

The unique globally stable solution of this system is the trajectory $\alpha(t) = \cos(\omega t + \phi)$, $\beta(t) = \sin(\omega t + \phi)$. Starting at the point $(\alpha, \beta) = (1, 0)$, we set $\phi = 0$, and we can thus use the α and β variables in order to eliminate the periodic time dependence from the original system. Note, however, that now even stationary solutions of the nonautonomous system have been transformed into limit cycles of the new bordered autonomous one. A further step to be carried out is the transformation of the continuation problem for a limit cycle (usually expressed as a Boundary Value Problem) into an algebraic problem such as (11). This step is performed automatically by numerical continuation tools through orthogonal collocation techniques (see, *e.g.*, [8], [3]).

B. Normal form analysis and bifurcations of limit-cycles

Loss of stability due to one or more multipliers leaving the unit circle can be also detected with continuation analysis, and it corresponds, by definition, to a bifurcation. Through the Center Manifold Projection Theorem it is possible to characterise the dynamics of the system in a neighborhood of the bifurcating limit cycle, reducing the system to the so

called *normal forms* of each bifurcation [14]. In particular, three situations are possible as far as bifurcations of limit cycles are concerned:

1) *Limit point of cycles bifurcation*. Before the bifurcation two limit cycles exist, with different stability properties. At the bifurcation they collide and disappear. Symmetries in the system can cause particular cases of this bifurcation, such as the *Pitchfork of cycles bifurcation*. In this case two scenarios are possible, *i.e.*, the supercritical one (before the bifurcation only a stable limit cycle exists, after the bifurcation two stable and one unstable limit cycles exist) and the subcritical one (before the bifurcation a stable and two unstable limit cycles exist, after the bifurcation only an unstable limit cycle exists).
2) *Period doubling bifurcation*. A limit cycle collides with another limit cycle that, at the bifurcation, has a doubled period: again, two scenarios are possible, the supercritical one (before the bifurcation only a stable limit cycle exists, after the bifurcation a period-doubled stable limit cycle and an unstable limit cycle exist) and the subcritical one (before the bifurcation the stable limit cycle and the unstable period-doubled limit cycles exist, after the bifurcation only an unstable limit cycle remains).
3) *Neimark-Sacker bifurcation*. A limit cycle collides at the bifurcation with an invariant torus (*i.e.*, a quasi-periodic invariant curve): also here two scenarios are possible, *i.e.*, the supercritical one (before the bifurcation only a stable limit cycle exists, after the bifurcation a stable invariant torus and an unstable limit cycle exist) and the subcritical one (before the bifurcation the stable limit cycle and an unstable invariant torus exist, after the bifurcation only an unstable limit cycle remains).

C. Bifurcation analysis of the magnetically controlled spacecraft

In order to investigate the behaviour of system (8)-(9) for increasing values of ε, the system is first bordered according to (12) with $\omega = 2\omega_0$. An additional issue to be dealt with in connection to (8)-(9) is the redundancy of the quaternion parameterisation. Indeed, (8)-(9) is an overdetermined dynamical system, since a dynamic equation can be substituted by the algebraic constraint $q_1^2+q_2^2+q_3^2+q_4^2 = 1$. So, in order to have a well defined differential problem, the order of the system must be reduced making explicit one of the elements of the quaternion vector. Note that as it is impossible to map completely the 3-sphere with an explicit function, analysis has to be confined to the positive hemisphere $q_4 > 0$ of the 3-sphere. Continuation results should then be analyzed in order to check that $q_4 \neq 0$ over the trajectories. Simulations will then be necessary in order to see the behaviors of trajectories in the neighborhood of the asymptotic state (see Section VI).

Practically, the problem can be solved through continuation tools, such as Auto [11] or MatCont [10]; the latter has been used in this study. As mentioned in the previous Section, in order to analyze asymptotic behaviors of the periodically forced system (8)-(9), we need to analyze periodic solutions of the corresponding bordered system. With reference to the numerical values of the parameters for the spacecraft model reported in Section VI, through continuation analysis the bifurcation diagram reported in Figure 2 was obtained, in which three different branches of limit cycles are shown.

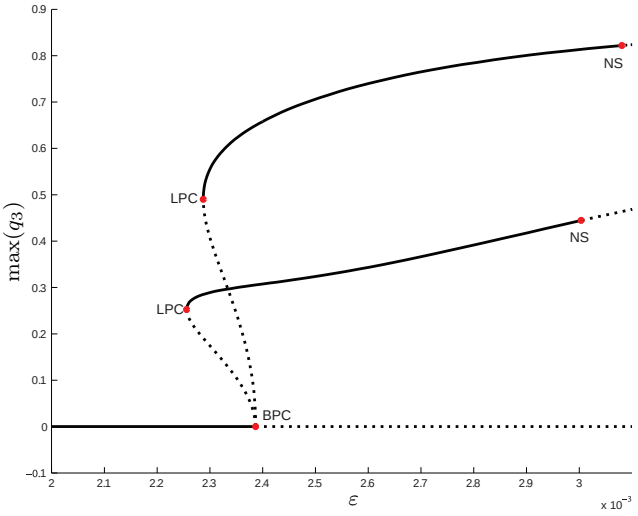

Fig. 2. Bifurcation diagram for the attitude dynamics of the magnetically controlled spacecraft: BPC - Branch Point of Cycles bifurcation; LPC - Limit Point of Cycles bifurcation; NS - Neimark-Sacker bifurcation.

In the central branch we have the stationary controlled solution, *i.e.*, the limit cycle of the bordered system associated with the equilibrium $(\bar{\boldsymbol{q}}, 0)$ for the original closed-loop system (8)-(9). As Floquet analysis has revealed, this solution is stable up to $\varepsilon = 2.386490 \times 10^{-3}$. At that value the solution undergoes a subcritical pitchfork bifurcation. From here, two non-trivial periodic unstable solutions depart, that give rise to the other two branches. The trivial limit-cycle loses its stability after the bifurcation and becomes a saddle limit cycle (with a one-dimensional unstable direction).

As mentioned above, normal form analysis reveals that two saddle limit cycles are involved in the pitchfork of cycle bifurcation. Following the upper branch, we see that the limit cycle (that increases in amplitude) undergoes a limit point of cycles bifurcation at $\varepsilon = 2.287454 \times 10^{-3}$, and then becomes stable. For further increasing values of ε, the stable limit cycle undergoes at $\varepsilon = 3.080625 \times 10^{-3}$ a supercritical Neimark-Sacker bifurcation. After the bifurcation a stable quasi-periodic invariant is born, as confirmed by the simulation results presented in Section VI.

Looking at the lower branch, also in this case the unstable limit cycle undergoes a limit point of cycles bifurcation at $\varepsilon = 2.255670 \times 10^{-3}$ and then becomes stable. Following the stable solution, the limit cycle undergoes a supercritical Neimark-Sacker bifurcation at $\varepsilon = 3.003435 \times 10^{-3}$, gener-

ating another stable invariant torus.

From the above analysis two interesting points can be made.

First, notice that relying only on Floquet analysis to determine the limiting value for ε may lead to erroneous conclusions. Indeed, the equilibrium $(\bar{\boldsymbol{q}}, 0)$ is the sole asymptotic solution for the system only up to $\varepsilon = 2.255670 \times 10^{-3}$, while the local approximation of the system reaches the stability boundary at the (larger) value $\varepsilon = 2.386490 \times 10^{-3}$. Therefore the bound $\varepsilon = 2.255670 \times 10^{-3}$ (more strict than the one obtained using Floquet analysis) should be considered for controller design purposes.

In addition, the analysis reveals that if $\varepsilon > 2.287454 \times 10^{-3}$ more than one asymptotic behavior is possible, depending on the initial conditions. In particular, for values of the scaling parameter such that $2.287454 \times 10^{-3} < \varepsilon < 2.386490 \times 10^{-3}$ the three attractors depicted in Figure 3 characterise the asymptotic behaviour of the closed-loop system.

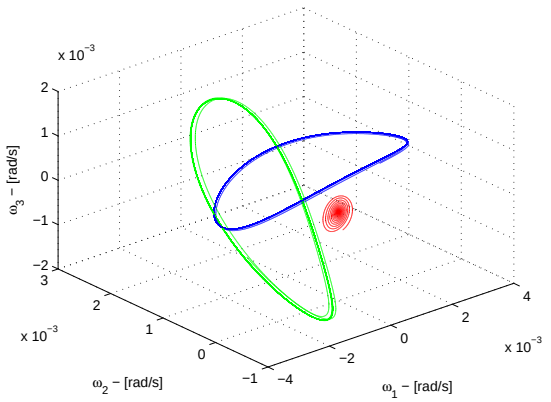

Fig. 3. Attractors (equilibrium and limit cycles) for $\varepsilon = 2.324 \times 10^{-3}$.

VI. SIMULATION RESULTS

In order to assess the time-domain behaviour of the magnetic attitude control law discussed in this paper, several simulated case studies have been considered.

The reference spacecraft has an inertia matrix given by $I = \text{diag}[27, 17, 25]$ kg m^2, and operates in a near polar (87^o inclination) orbit with an altitude of 450 km and a corresponding orbit period of about 5600 s. The controller parameters are given by $k_p = k_v = 50$.

For the considered spacecraft, first three simulations have been carried out with $\varepsilon = 2.324 \times 10^{-3}$, in order to illustrate that in this case three attractors can characterise the asymptotic behaviour of the system, depending on the initial conditions. Indeed, Figure 4 depicts a trajectory for the state variables of the closed-loop system which converge to the desired equilibrium, while, on the other hand, Figures 5 and 6 illustrate trajectories converging to the stable limit cycles associated to the upper and the lower branches, respectively,

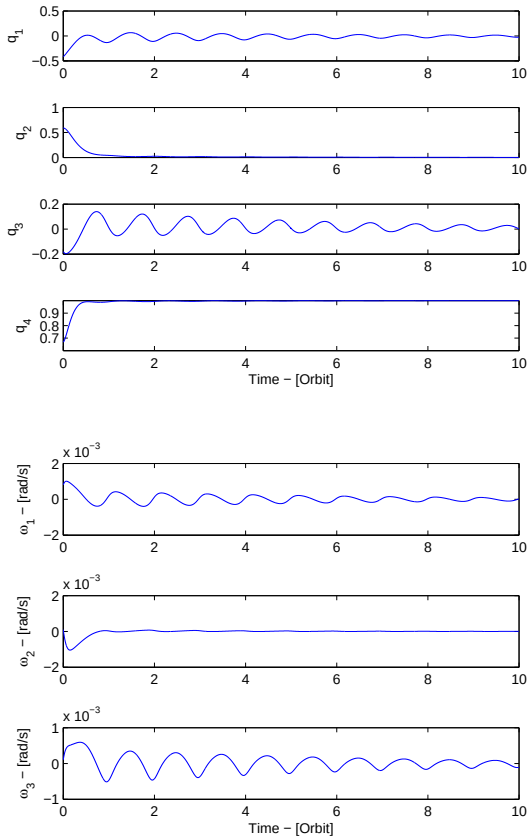

Fig. 4. Quaternion and angular rates for $\varepsilon = 2.2324 \times 10^{-3}$: initial state leading to a trajectory converging to the equilibrium.

of the bifurcation diagram in Figure 2. Note that for the computed trajectories the condition $q_4 > 0$ actually holds.

Finally, a simulation has been carried out with $\varepsilon = 3.1 \times 10^{-3}$ to illustrate the convergence of the solution to a stable torus, as predicted by the analysis for this value of the scaling parameter. The time-domain representation of the solution is depicted in Figure 7, from which the presence of multiple frequencies in the oscillation of the state variables can be seen. Figure 8 on the other hand shown a 3D representation of the torus and the associated Poincare' map.

VII. CONCLUDING REMARKS

In this paper the dynamics of a spacecraft equipped with magnetic actuators operating under a static attitude and rate feedback control law designed using averaging theory has been considered and the problem of determining the asymptotic behaviour of the closed-loop system as a function of the averaging scaling parameter has been analysed, using bifurcation methods. The results provide an accurate assessment of the maximum value of the scaling parameter for which the closed-loop system exhibits the desired equilibrium as sole asymptotic behaviour and a catalogue of other possible attractors for the range of practical interest of the parameter.

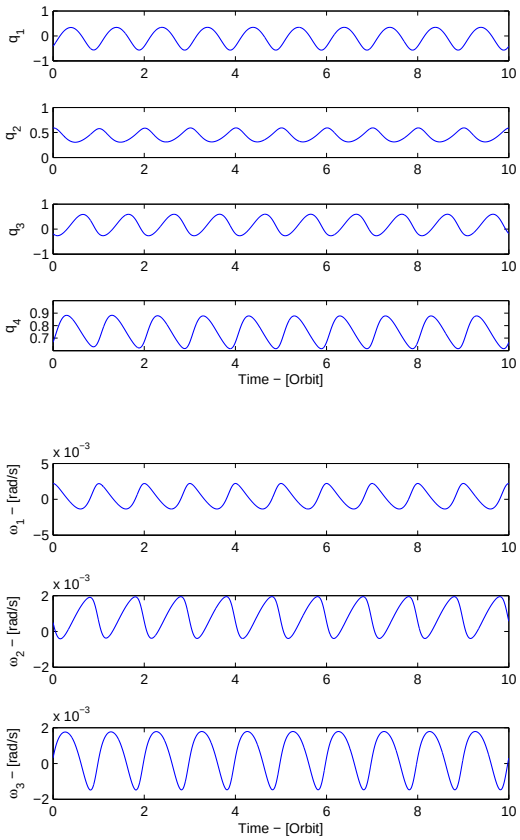

Fig. 5. Quaternion and angular rates for $\varepsilon = 2.2324 \times 10^{-3}$: initial state leading to a trajectory converging to the upper branch limit cycle.

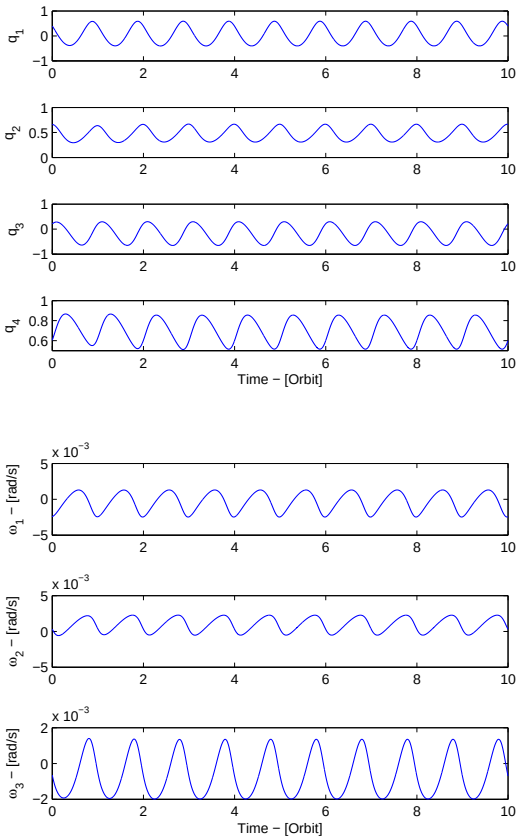

Fig. 6. Quaternion and angular rates for $\varepsilon = 2.2324 \times 10^{-3}$: initial state leading to a trajectory converging to the lower branch limit cycle.

REFERENCES

[1] E.L. Allgower and K. Georg. *Numerical Continuation Methods: An Introduction*. Berlin, 2000.

[2] C. Arduini and P. Baiocco. Active magnetic damping attitude control for gravity gradient stabilised spacecraft. *Journal of Guidance and Control*, 20(1):117–122, 1997.

[3] U.C. Ascher, R.M.M. Mattheij, and B. Russell. *Numerical Solution of Boundary Value Problems for Ordinary Differenital Equations*. Philadelphia, 1995.

[4] S.P. Bhat and A.S. Dham. Controllability of spacecraft attitude under magnetic actuation. In *IEEE Conference on Decision and Control, Maui, Hawaii, USA*, 2003.

[5] S. Bittanti and P. Colaneri. *Periodic Systems: Filtering and Control*. Springer, 2008.

[6] L.Q. Chen and Y.Z. Liu. Chaotic attitude motion of a magnetic rigid spacecraft and its control. *International Journal of Non-Linear Mechanics*, 37(3):493–504, 2002.

[7] C. J. Damaren. Comments on "Fully magnetic attitude control for spacecraft subject to gravity gradient". *Automatica*, 38(12):2189, 2002.

[8] C. de Boor and B. Swartz. Collocation at gaussian points. *SIAM Journal of Numerical Analysis*, 10:582606, 1973.

[9] P. Deuflhard, B. Fiedler, and P. Kunkel. Efficient numerical pathfollowing beyond critical points. *SIAM Journal of Numerical Analysis*, 24:912927, 1987.

[10] A. Dhooge, W. Govaerts, and Yu. A. Kuznetsov. MATCONT: A MATLAB package for numerical bifurcation analysis of ODEs. *ACM Trans. Math. Software*, 29(2):141–164, 2003. `http://sourceforge.net/projects/matcont`.

[11] E. J. Doedel, A. R. Champneys, F. Dercole, T. F. Fairgrieve, Yu. A. Kuznetsov, B. Oldeman, R. C. Paffenroth, B. Sandstede, X. J. Wang, and C. H. Zhang. AUTO-07p: Continuation and bifurcation software for ordinary differential equations. Department of Computer Science, Concordia University, Montreal, QC, 2007.

[12] H.A. Fujii, W. Ichiki, S. Suda, and T.R. Watanabe. Chaos analysis of librational control of gravity-gradient satellite in elliptic orbit. *Journal of Guidance, Control and Dynamics*, 23(1):145–146, 2000.

[13] J. Kuang, S. Tan, and A.Y.T. Leung. Chaotic attitude tumbling of an asymmetric gyrostat in a gravitational field. *Journal of Guidance, Control and Dynamics*, 25(4):804–814, 2002.

[14] Yu. A. Kuznetsov. *Elements of Applied Bifurcation Theory*. Springer-Verlag, New York, 2004. 3rd ed.

[15] M. Lovera and A. Astolfi. Spacecraft attitude control using magnetic actuators. *Automatica*, 40(8):1405–1414, 2004.

[16] M. Lovera and A. Astolfi. Global magnetic attitude control of spacecraft in the presence of gravity gradient. *IEEE Transactions on Aerospace and Electronic Systems*, 42(3):796–805, 2006.

[17] M. Lovera, E. De Marchi, and S. Bittanti. Periodic attitude control techniques for small satellites with magnetic actuators. *IEEE Transactions on Control Systems Technology*, 10(1):90–95, 2002.

[18] H. G. E. Meijer, F. Dercole, and B. E. Oldeman. Numerical bifurcation analysis. In Robert A. Meyers, editor, *Encyclopedia of Complexity and System Science*, pages 6329–6352. 2009.

[19] M. Psiaki. Magnetic torquer attitude control via asymptotic periodic linear quadratic regulation. *Journal of Guidance, Control and Dynamics*, 24(2):386–394, 2001.

[20] E. Silani and M. Lovera. Magnetic spacecraft attitude control: A survey and some new results. *Control Engineering Practice*, 13(3):357–371, 2005.

[21] P. Wang and Y. Shtessel. Satellite attitude control using only magnetic torquers. In *AIAA Guidance, Navigation, and Control Conference and Exhibit, Boston, USA, 1998*, 1998.

[22] J. Wertz. *Spacecraft attitude determination and control*. D. Reidel Publishing Company, 1978.

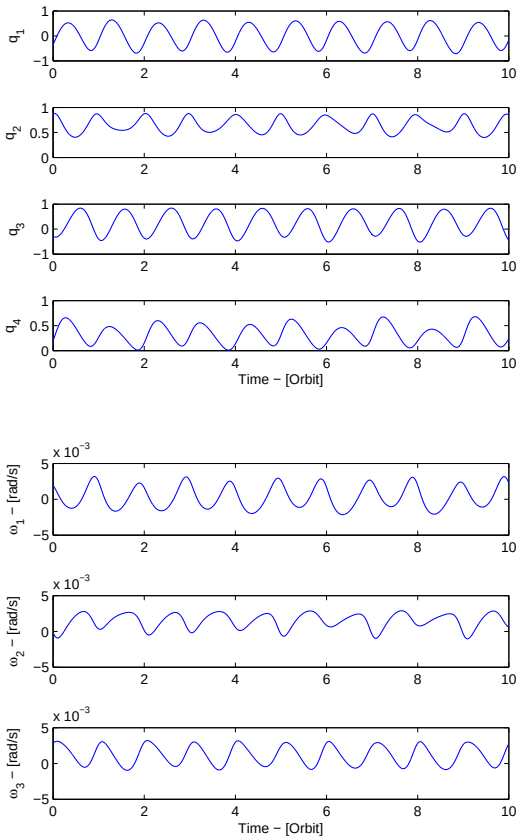

Fig. 7. Quaternion and angular rates for $\varepsilon = 3.1 \times 10^{-3}$: initial state leading to a trajectory converging to the stable torus.

[23] R. Wisniewski and M. Blanke. Fully magnetic attitude control for spacecraft subject to gravity gradient. *Automatica*, 35(7):1201–1214, 1999.

[24] R. Wisniewski and J. Stoustrup. Periodic H_2 Synthesis for Spacecraft Attitude Control with Magnetorquers. *Journal of Guidance, Control and Dynamics*, 27(5):874–881, 2004.

[25] A. Zanchettin and M. Lovera. H_∞ attitude control of magnetically actuated satellites. In *IFAC World Congress, Milano, Italy*, 2011.

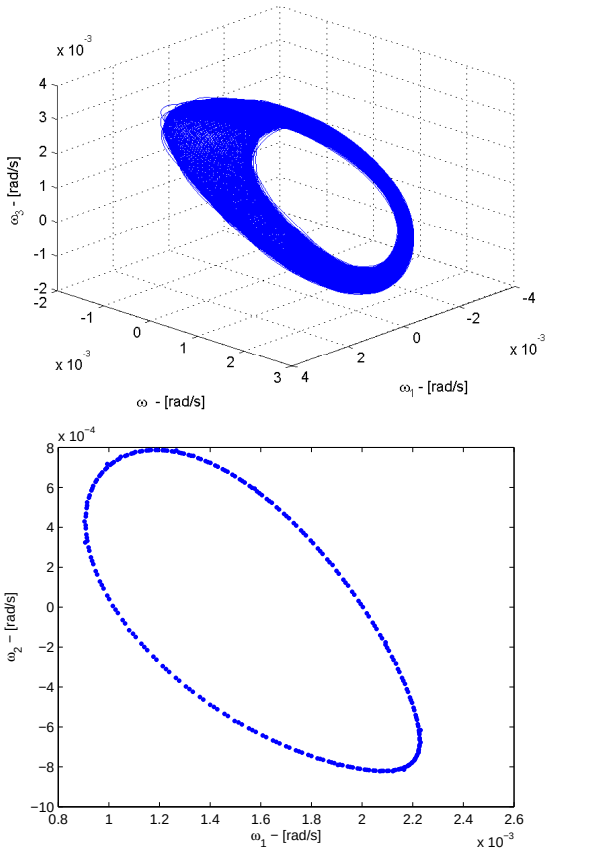

Fig. 8. Top: 3D plot of the torus. Bottom: Poincare' map for the torus.